Strong Excitonic Interactions in the Oxygen-Reducing Site of *bd*-Type Oxidase: The Fe-to-Fe Distance between Hemes *d* and b_{595} is 10 Å†

Alexander M. Arutyunyan,§ Vitaliy B. Borisov,§ Vladimir I. Novoderezhkin,§ Josh Ghaim,‡ Jie Zhang,‡ Robert B. Gennis,‡ and Alexander A. Konstantinov*,§

A.N. Belozersky Institute of Physico-Chemical Biology, Lomonosov Moscow State University, 119991 Moscow, Russia, and Department of Biochemistry, University of Illinois, 600 S. Mathews Street, Urbana, Illinois 61801

Received September 14, 2007; Revised Manuscript Received December 6, 2007

ABSTRACT: Absorption and circular dichroism (CD) spectra of cytochrome *bd* from *Escherichia coli* have been compared for the wild type enzyme and an inactive mutant in which a highly conserved E445 in subunit I has been replaced by alanine [Zhang, J., Hellwig, P., Osborne, J. P., Huang, H. W., Moenne-Loccoz, P., Konstantinov, A. A., and Gennis, R. B. (2001) *Biochemistry 40*, 8548−8556]. The absorption bands of ferrous heme b_{595} are absent from the spectrum of the dithionite-reduced E445A form of cytochrome *bd*. The difference between the spectra of the dithionite-reduced WT and E445A enzymes indicates that in the mutant, heme b_{595} is present but is not reducible by dithionite. Cytochrome *bd* reveals intense CD signals dominated by heme *d*, with almost no contribution from heme b_{595} or heme b_{558}. The CD spectrum of the reduced wild type enzyme in the Soret band indicates strong excitonic interactions between ferrous heme *d* and ferrous heme b_{595}, and these interactions are not observed in dithionite-reduced E445A mutant, in which heme b_{595} remains in the ferric state. Modeling the excitonic interactions in both absorption and CD spectra has been carried out, yielding an estimate of the Fe-to-Fe distance between heme *d* and heme b_{595} of about 10 Å. The physical proximity supports the hypothesis that heme *d* and heme b_{595} can form a di-heme oxygen reducing site, a unique structure for respiratory oxidases.

Cytochrome *bd* is one of two terminal oxidases in the respiratory chain of *Escherichia coli* (reviewed in refs *1*−*3*). The enzyme oxidizes ubiquinol or menaquinol and reduces oxygen to water. For each electron transferred from quinol to oxygen, the proton from the quinol is released to the outside, whereas the proton required for water formation from oxygen is taken up from the inside. Therefore, the reaction is coupled to generation of membrane potential and ΔpH across the membrane (*4*−*6*, *7*).

The *bd*-type oxidases are not found in eukaryotes but are widely distributed in prokaryotes, particularly in pathogenic bacteria, and have distinct physiological roles (*3*). For example, the high affinity for oxygen of the *bd*-type oxidases allows aerobic bacteria to grow under conditions of limited oxygen supply (*8*, *9*). Similarly, cytochrome *bd* is utilized by anaerobic bacteria to scavenge traces of ambient oxygen that might be toxic under conditions of incomplete anaerobiosis (*10*). Depleting intracellular O_2 through cytochrome *bd* enables aerotolerant dinitrogen fixation in *Azotobacter vinelandii* and other bacteria (*11*−*14*). In recent years, evidence has accumulated that expression of *bd*-type oxidases is important for the virulence of pathogens responsible for tuberculosis (*15*), bacillary dysentery (*16*), brucellosis (*17*, *18*), infection by Group B *Streptococcus* (*19*), and *Salmonella* infection (*20*) as cytochrome *bd* allows bacteria to colonize oxygen-poor habitats inside the host as well as to resist the host immune response.

Despite the growing interest in the physiological role of cytochrome *bd*, the structure and catalytic mechanism of the *bd*-family of oxidases have been explored significantly less than for the heme-copper oxidases. In general, the *bd*-type quinol oxidases catalyze the same chemical reaction as do the heme-copper oxidases, i.e., reducing O_2 to $2H_2O$. However, there is no structural homology between the *bd*-type oxidases and the heme-copper oxidase superfamily. Cytochrome *bd* is a heterodimeric membrane protein with one copy of each of two subunits (CydA, 57kDa; CydB, 43 kDa). There are three heme prosthetic groups, heme b_{558}, heme b_{595}, and heme *d*, but no copper in the *bd*-type oxidases. There is no crystal structure for any of the *bd*-type oxidases, but genetics and spectroscopic methods have provided data in support of a model that predicts that all the three heme prosthetic groups are located close to the outer side of the membrane (*21*).

The mechanisms of quinol oxidation, intraprotein electron transfer, and subsequent reduction of oxygen to water remain essentially unknown. The low spin heme b_{558} is believed to be the electron entry point to the quinol oxidation site, and the high spin heme *d* is the site involved in binding and reducing O_2 to H_2O. The functional role of the third redox center, a high-spin heme b_{595}, is least understood. Heme b_{595}

† This work was supported by the International Scholar Awards from the Howard Hughes Medical Institute 55005615 and 55000320 (A.A.K.), grant CGP-2836 from Civilian Fund for Research and Development (A.A.K., R.B.G.), the Russian Foundation for Basic Research grants 05-04-48096 (V.B.B.) and 06-04-48917 (V.I.N.), and grant from the National Institutes of Health, HL16101 (R.B.G.)

* To whom correspondence should be addressed. Tel.: +7-495-9395549; fax: +7-495-9393181; e-mail: konst@genebee.msu.su.

§ Lomonosov Moscow State University.

‡ University of Illinois.

10.1021/bi701884g CCC: $40.75
Published on Web 01/19/2008

had been proposed to operate simply as an electron carrier between heme b_{558} and heme *d* (*22*, *23*). Alternatively, heme b_{595} might be directly involved in the chemistry of O_2 reduction as first considered by Rothery et al. (*24*). It has been proposed that heme *d* and heme b_{595} form a di-heme oxygen reducing center, functionally analogous to the heme a_3/Cu_B bimetallic center in the heme-copper oxidases (*25*, *26*).

There are several lines of evidence supporting or consistent with models in which heme *d* and heme b_{595} are physically close to each other.

(1) Photoinduced dissociation of CO from ferrous heme *d* perturbs the absorption spectrum of heme b_{595} on a subpicosecond time scale, implicating direct electronic/steric interaction between the two hemes (*27*, *28*).

(2) FTIR studies have indicated that under certain circumstances, CO which is photodissociated from heme *d* in a frozen sample can transiently bind to heme b_{595} before rebinding to heme *d* (*25*). This suggests a pathway within the protein from the iron of heme *d* to that of heme b_{595} that is available even at low temperatures.

(3) The ligand-binding behavior of cytochrome *bd* under static conditions is peculiar (*1*, *25*, *26*, *29*−*31*). As expected for a high-spin heme, heme *d* binds exogenous heme iron ligands in the ferric and/or ferrous states (e.g., O_2, CO, NO, CN^-, H_2O_2). However, heme b_{595}, though also high-spin, does *not* react to any significant extent with these exogenous ligands, which is unusual. One explanation that has been suggested is that the binding of an exogenous ligand to heme *d* precludes binding of a second ligand molecule to heme b_{595} due to anticooperative interactions (*31*, *32*). The general implication is that the two redox centers share a common heme-binding pocket that can accommodate only one molecule of the exogenous ligand.

(4) Recent experiments indicate that the hemes b_{595} and *d* may be electrostatically coupled to the same pair of redox-linked ionizable groups (*33*), which is most easily explained by the two hemes being physically close to each other.

Recently, it was shown that the replacement of a highly conserved glutamate 445 by Ala or Gln results in expression of enzymatically inactive cytochrome *bd* that selectively maintains heme b_{595} in the oxidized form, even in the presence of dithionite, while not affecting either heme b_{558} or heme *d* (*33*). Initially, it was thought that heme b_{595} was absent from the mutants (*34*), but subsequent work showed that the heme is locked in the oxidized state because one of the two redox-dependent heme-linked ionizable groups coupled to both hemes b_{595} and *d* is lost in the mutant (*33*).

The E445A mutant provides a unique opportunity to resolve the contribution of the ferrous heme b_{595} to the spectral characteristics of reduced cytochrome *bd* and facilitates an investigation into the potential electronic interactions between ferrous heme b_{595} and other iron-porphyrin components within the *bd*-type quinol oxidase. In this work, the circular dichroism (CD[1]) and absorption spectra of the E445A mutant are compared with the spectra of the wild type enzyme. CD spectroscopy reveals strong electronic interactions (excitonic/dipole−dipole) between electronic transitions of ferrous heme *d* and ferrous heme b_{595} in the Soret band of the reduced wild type enzyme. The interactions are lost in the dithionite-reduced E445A mutant in which heme b_{595} remains ferric and, hence, absorbs at significantly shorter wavelength. Modeling the excitonic interaction in the absorption and CD spectra yields an estimate of the Fe-to-Fe distance between the two hemes as ~10 Å. The data provide direct evaluation of the proximity of the heme *d* and heme b_{595} and provide a firm basis for the hypothesis on the cooperation of the two hemes in the reduction of dioxygen to water.

MATERIALS AND METHODS

Strains and Biochemical Protocols. E. coli strain GO 105/pTK1 lacking cytochrome bo_3 and overexpressing cytochrome *bd* (*35*) was used to isolate wild type cytochrome *bd* (*36*). The E445A mutant was obtained as detailed in ref *34*. The "L65C" mutant oxidase has all six endogenous cysteines replaced by either serine or alanine (subunit I: C128A, C396S, and C479A; subunit II: C214S, C301S, and C358S), plus a cysteine introduced in subunit I (L65C). The mutant is partially active *in vivo* but is not stable upon solubilization and purification. Hemes are easily lost during purification, and the final heme composition depends on the preparation. The preparation used in the current work had no heme *d* but did contain both heme b_{558} and heme b_{595}.

Spectroscopy. Absorption spectra were recorded using a computer-interfaced Aminco-SLM DW 2000 UV−vis spectrophotometer modified in the laboratory of Dr. Arutyunyan in A.N. Belozersky Institute, Moscow State University. CD spectra were recorded in a computer-interfaced dichrograph Mark V (Jobin Yvon, France) upgraded by Dr. Arutyunyan. Data processing and simulation of the spectra were performed with the aid of graphics programs RDA and WTEST developed by I. Khomenkov and A. M. Arutyunyan. All spectroscopic measurements were performed at room temperature using 50 mM HEPES/50 mM CHES buffer, 0.5 mM EDTA, pH 8.0, containing 0.025% of sodium *N*-lauroylsarcosinate.

Normalization of the Spectra. The concentration of the wild type cytochrome *bd* is often determined from the dithionite-reduced *minus* air-oxidized difference absorption spectrum using the value of $\Delta\epsilon_{628-607} = 10.8\ mM^{-1}\ cm^{-1}$ (*31*). This coefficient corresponds to $\Delta\epsilon_{630-670}$ of $25\ mM^{-1}\ cm^{-1}$ for the absolute spectrum of the dithionite-reduced sample, which also can be used to quantify the enzyme (*33*). In this work, the absolute spectra were used to normalize the concentrations of the wild type and E445A mutant oxidases, since the difference spectrum is too sensitive to variations in the fraction of the oxygenated form of the enzyme in the "as isolated" preparation, and this fraction is not the same for the wild type and mutant.

In order to quantitatively compare the absorption spectra of the wild type and E445A forms of cytochrome *bd*, the amplitude of the ferrous heme *d* absorption band at 630 nm in the absolute spectra of the dithionite-reduced samples was used to normalize the spectra. Close inspection shows that the line shapes of the 630 nm absorption bands of heme *d* in the wild type and mutant oxidases are not quite identical (Figure 1). In the spectrum of the E445A mutant the band is broader on the blue side of the maximum. However, the line shapes on the red side of the 630 nm absorption bands are

[1] Abbreviations: CD, circular dichroism; MCD, magnetic circular dichroism.

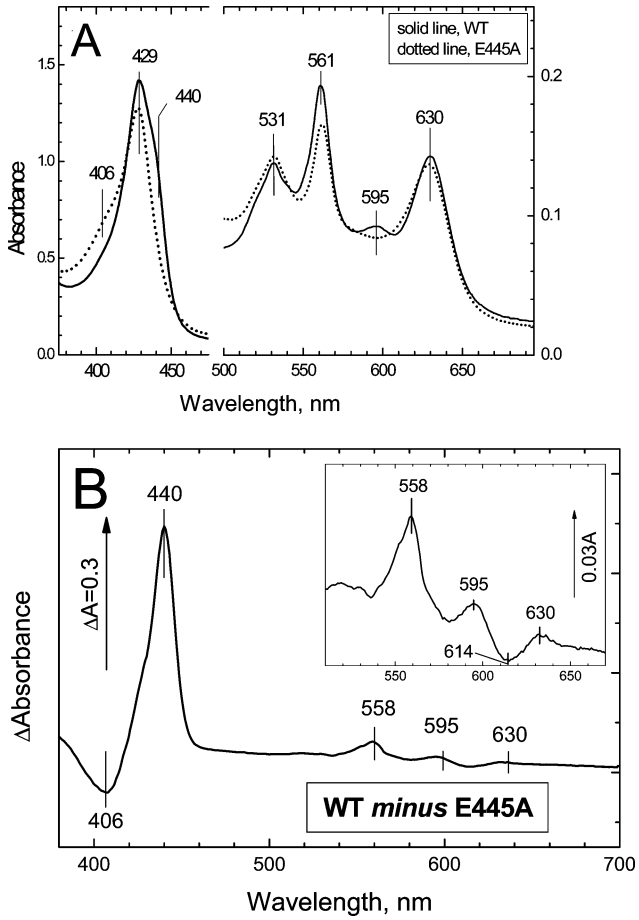

FIGURE 1: Absorption spectra of cytochrome *bd*. (A) Absolute spectra of the dithionite-reduced wild type (solid line) and E445A mutant enzyme (dotted line). (B) The difference between the normalized absorption spectra of the wild type and E445A mutant enzymes. The inset shows a magnified view of the visible region. The spectra are recorded at room temperature in 50 mM HEPES/50 mM CHES buffer, 0.5 mM EDTA, pH 8.0, and 0.025% sodium *N*-lauroylsarcosinate. Concentration of wild type cytochrome *bd* was 4.5 μM. The spectrum of the E445A mutant was normalized to the spectrum of wild type enzyme by the 630 nm absorption band of heme *d*, as described in the text.

virtually identical for the wild type and mutant enzymes. Therefore, the intensities of the ferrous heme *d* absorption were determined using the wavelength pair 630 nm-*minus*-670 nm instead of the commonly used pair 630 nm-*minus*-607 nm. The results obtained with this method were consistent within ~5% with those obtained using the intensity of the MCD spectral component assigned to ferrous heme b_{558} and the intensity of the CD band of the ferrous heme *d* (Figure 2A). The concentration of the L65C mutant was determined from the dithionite-reduced absolute absorption spectra using the value of $\Delta\epsilon_{531} = 9$ mM^{-1} cm^{-1} for the heme b_{558} β-band, measured versus a baseline connecting the points at 505 and 544 nm.

RESULTS AND DISCUSSION

Absorption Spectra of Wild Type and E445A Cytochrome bd. Absolute absorption spectra of reduced cytochrome *bd* from the wild type and E445A mutant oxidases are compared in Figure 1A. The absorption bands of heme *d* (630 nm) and heme b_{558} (561 and 531 nm) are retained by the mutant. However, the absence of the 595 nm band, a marked decrease of the peak at 561 nm and the disappearance of the shoulder at ~440 nm in the Soret region indicate the loss of the contribution from reduced heme b_{595} to the absorption spectrum of the mutant. Similar observations were made previously (*34*) and led to the proposal that E445A replacement results in a loss of heme b_{595}. However, if heme b_{595} were absent in the mutant, the difference between the normalized absorption spectra of the dithionite-reduced wild type and E445 oxidases should give an absolute spectrum of ferrous heme b_{595}. The difference spectrum resulting from the subtraction of the spectra in Figure 1A is shown in Figure 1B. All three bands characteristic of the ferrous heme b_{595} in the visible with the maxima at 630, 595, and 558 nm (cf. refs *37*, *38*) are present, and an asymmetric band at 440 nm in the Soret is observed (cf. ref *27*). However, the difference spectrum in Figure 1B has a pronounced negative band at 406 nm, on the blue side of the Soret peak from ferrous heme b_{595}, as well as a trough at 614 nm in the visible. Negative extrema are not expected and are inconsistent with the hypothesis that the spectroscopic difference is simply the result of the absence of heme b_{595} from the mutant. The difference spectrum in Figure 1B is, on the other hand, consistent with a reduced-*minus*-oxidized difference spectrum of heme b_{595}, rather than with the absolute spectrum of the ferrous b_{595}. Thus, careful inspection of the absorption spectra shows, in agreement with ref *33*, that heme b_{595} is not missing in the E445A mutant form of cytochrome *bd*. Rather, the heme is retained but cannot be reduced by dithionite as demonstrated previously by EPR spectroscopy (*33*).

CD Spectra of the Wild Type and E445A Mutant Oxidases: Excitonic Interactions between Ferrous Heme d and Heme b_{595}. To the best of our knowledge, optical activity of cytochrome *bd* was not studied earlier. The CD spectrum of fully reduced wild type cytochrome *bd* (Figure 2A**,** solid curve) is characterized by a maximum at 629 nm, close to the absorption peak of ferrous heme *d*, and by a strong asymmetric signal in the Soret with an intense negative band near 440 nm, a zero crossing point at 426 nm, and a minor positive extremum at 416 nm with a shoulder at 397 nm. The peak-to-trough intensity of the CD spectrum in the Soret (~400 M^{-1} cm^{-1}) is exceptionally high for hemoproteins with either a single (e.g., cytochrome *c* or myoglobin) or multiple, weakly interacting hemes (e.g., hemoglobin). Typically, values of $\Delta\epsilon_{R-L}$ are usually in the range of 10−50 mM^{-1} cm^{-1} (*39*, *40*). Air-oxidized cytochrome *bd* (referred to as the "as isolated" state) contains a mixture of redox forms, dominated by the oxy-complex ($b^{3+}{}_{558}$,$b^{3+}{}_{595}$,d^{2+}-O_2), and it is the characteristics of the heme d^{2+} oxy-complex with the far-red band shifted to 645 nm (inset) that dominates the CD spectrum of air-oxidized cytochrome *bd*.

These data and detailed circular dichroism studies of cytochrome *bd* complexes with various ligands of heme *d* in the ferrous and ferric state, such as O_2, H_2O_2, CO, NO, and CN^- (Borisov, Arutyunyan, Zhang, Gennis, and Konstantinov, manuscript in preparation) indicate that the CD spectrum of cytochrome *bd* is dominated by the optical activity of heme *d*, whereas heme b_{558} and heme b_{595} contribute but little. The high ellipticity of heme *d* is not surprising because of the decreased symmetry of the chlorin macrocycle and the strong splitting of the B_{00} and Q_{00} transitions of heme *d* into the *x* and *y* components (*41*, *42*), whereas those transitions are nearly degenerate in the

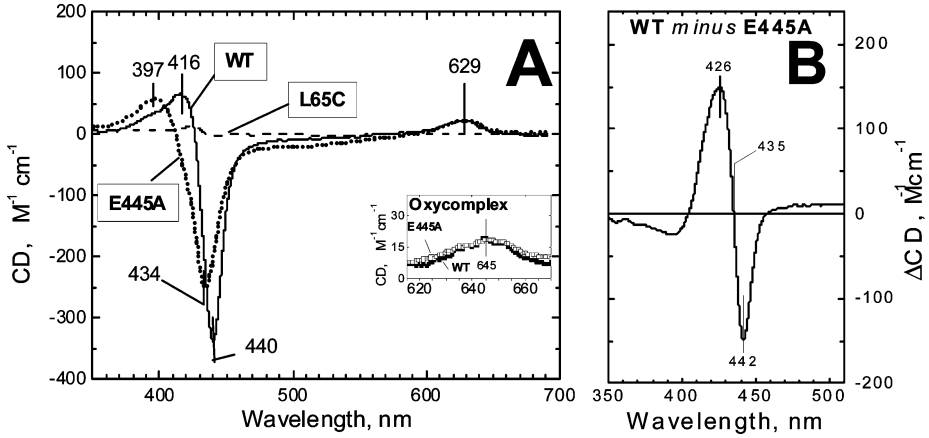

FIGURE 2: Circular dichroism spectra of dithionite-reduced wild type and E445A mutant cytochrome *bd* recorded at room temperature in 50 mM HEPES/50 mM CHES buffer, 0.5 mM EDTA, pH 8.0, and 0.025% sodium *N*-lauroylsarcosinate. (A) Absolute spectra of the wild type cytochrome *bd* (solid line), E445A mutant (dotted line), and the L65C mutant (dashed line) which lacks heme *d* but contains heme b_{558} and heme b_{595}. The spectra were normalized by enzyme concentration as described in Materials and Methods. The concentration of the L65C mutant was 6.5 μM. The inset shows the near-IR band of heme *d* from the spectrum of the air-oxidized wild type and E445A forms of the enzyme. (B) Difference between the CD spectra of the wild type and E445A mutant in the Soret region.

protoheme-containing heme b_{558} and heme b_{595} components of the enzyme. This conclusion can be illustrated by the CD spectrum of the reduced L65C mutant of cytochrome *bd* which contains both heme b_{558} and heme b_{595} but lacks heme *d* (Figure 2A**,** dashed line).

The CD spectra of the E445A mutant are shown in Figure 2 (dotted lines). In the far red region, the CD spectra of the E445A mutant and wild type enzyme are virtually identical, both in the dithionite-reduced (main panel) and air-oxidized states (inset). This observation is in good agreement with the data from absorption spectroscopy and shows that the intrinsic optical characteristics of heme *d* are not altered significantly by the E445A replacement. At the same time, dramatic changes are induced by the mutation in the Soret region. The spectrum decreases in magnitude and shifts to the blue.

The difference between the CD spectra of the dithionite-reduced wild type and E445A oxidases (Figure 2B) yields a bilobe derivative-shaped curve centered at 435 nm with an amplitude ($\sim$300 M^{-1} cm^{-1}) close to that of the parent CD spectra. A derivative-shaped CD signal of such intensity is unprecedented for an isolated heme in a protein (*39*, *40*). The induced CD signals of globins or heme peptide complexes are usually much smaller ($<$50 M^{-1} cm^{-1}) and are very asymmetric (*43*−*47*).

On the other hand, a large magnitude, bilobed signal is expected for exciton splitting of the electronic transitions of two interacting chromophores. Such interactions have been observed in the CD spectra of the di-heme cytochromes *b* from chromaffine granule (*48*), in respiratory chain Complex II (*49*) and Complex III (*50*) and in the chloroplast Complex b_6f (*51*) (see ref *40* for a survey and analysis). It is reasonable to conclude, therefore, that the intense CD difference spectrum in Figure 2B is due to excitonic interaction between the reduced hemes b_{595} and *d* in the wild type cytochrome *bd*. These interactions are abolished in the E445A mutant because heme b_{595} remains oxidized.

Modeling the Excitonic Interactions between Heme b_{595} *and Heme d: Estimating the Distance between the Heme* b_{595} *and Heme d.* The contribution of the exciton coupling to the absorption and CD spectra was modeled for dithionite-reduced cytochrome *bd* in the Soret region (350 to 500 nm). A standard exciton model was used (*52*), considering the B_x and B_y transitions for each heme *d* and heme b_{595}. The model takes into account intermolecular coupling, energetic (diagonal) disorder due to site inhomogeneity, and homogeneous line broadening due to the interaction with the surroundings. The approach is similar to that of Palmer and Esposti (*40*), who modeled the CD spectra of several di-heme cytochromes *b* in the Soret region. In the work of Palmer's group, the two orthogonally polarized B_x and B_y transitions of both *b* hemes were assumed to be isoenergetic and to have the same dipole strength of 21.5 D^2, giving the total dipole strength of the Soret band of 43 D^2. The line widths necessary to explain the experimental CD spectra were 500−700 cm^{-1} (fwhm). The choice of the initial parameters used for the fitting in the current work was modified as follows.

(1) Ferrous Heme b_{595}. The Soret band of b_{595}^{2+} in the absence of excitonic interactions has been approximated provisionally by two nearly degenerate B_{xy} transitions at 436.7 and 437.3 nm, located between the exciton-split bands of b_{595}^{2+} at ca. 441 and 434 nm which are observed experimentally in the reduced wild type enzyme (see Figure 1D in (*27*)). The total dipole strength of the Soret band of different *b*-type cytochromes varies in the range 41−125 D^2 (4.1−12.5·10^{-35} cgs units) (*40*, *48*). A value of 70 D^2 was chosen in this work by comparison of the spectral characteristics of heme b_{595} with those of myoglobins and peroxidases.

(2) Ferrous Heme d^{2+}. The Soret band of heme *d* is buried within the much stronger absorption bands of heme b_{558} and heme b_{595}. The following considerations were taken into account to deduce the characteristics of ferrous heme *d*.

(i) Estimating the Position of the Ferrous Heme d Soret Transitions. Significant splitting between the B_x and B_y transitions is expected for chlorin-type heme *d* due to asymmetry of its macrocycle (typically, around 10 nm, cf. refs *41*, *42*, *53*). It is reasonable to assume that in the absence of excitonic interactions with ferrous heme b_{595}, the Soret band of heme d^{2+} is dominated by a transition at $\sim$434 nm. The assumption is based on three observations. First,

photodissociation of CO from the mixed valence complex of wild type cytochrome *bd* (b^{3+}_{558} b^{3+}_{595} d^{2+}-CO) results in the appearance of an absorption band of free heme d^{2+} at 434−435 nm on a picosecond time scale (*27*, *28*). Second, CO binding to ferrous heme d^{2+} in the dithionite-reduced E445A mutant ($b^{2+}_{558}b^{3+}_{595}d^{2+}$) results in bleaching of an absorption band at 434 nm (Borisov, Zhang, Arutyunyan, Gennis, Konstantinov, manuscript in preparation). Third, the CD spectrum of the E445A mutant, which is dominated by the contribution of heme d^{2+}, has a strong negative Gaussian at 434 nm in the dithionite-reduced state (Figure 2A, dotted line).

This major optical band at 434 nm of heme d^{2+} is assigned to the B_y transition. Deconvolution of the dithionite-reduced E445A CD spectrum gives, in addition to the strong negative band at 434 nm ($\Delta\epsilon_{R-L}$ of 250 mM^{-1} cm^{-1}), three weaker positive Gaussians centered at ca. 426, 405, and 395 nm ($\Delta\epsilon_{R-L}$ of 27, 32, and 66 mM^{-1} cm^{-1}, respectively, data not shown). Of these, it is only the component at 426 nm that is within a reasonable energy from the 434 nm band (the B_y transition) to be assigned to the B_x transition. The assignment is consistent with the shoulder at 426 nm observed in the spectrum of heme d^{2+} in the picosecond CO-photodissociation/geminate recombination experiments (*27*). This shoulder is most clearly seen in the difference between spectra a and b in Figure 2B in ref *27*. A separation of 8 nm between the B_x and B_y transitions is in good agreement with the Soret band splitting observed in the absorpion spectra of chlorine model compounds and chlorin-reconstituted proteins (e.g., refs *41*, *42*, *53*).

The origin of the two other minor Gaussians (at 405 and 395 nm) in the CD spectrum of the dithionite-reduced E445A mutant is not clear. These transitions may be associated with ferric heme b_{595} or with vibronic components of the Soret band.

(ii) Estimating the Transition Strength of the Ferrous Heme d Soret Band. The Soret band of heme *d*-containing proteins is typically 2−3-fold weaker than in protoheme proteins (*41*, *42*, *53*). Taking the absorption spectrum of iron-octaethylchlorin pyridine hemochromogen as a model (see Figure 1C in ref *41*), total dipole strength of the Soret band of heme *d* is estimated to be about 1/3 that of heme b_{595}. As noted above, the dipole strength of the shorter wavelength B_x transition in heme *d* is likely to be several-fold weaker than for the B_y band.

With these considerations in mind, the optical characteristics of the Soret band of cytochrome *bd* were modeled as follows.

Electronic Transitions in the Dithionite-Reduced Wild Type Cytochrome bd. The intrinsic (noninteracting) B_x (heme *d*), B_y (heme *d*), B_x (heme b_{595}), and B_y (heme b_{595}) transitions center at 426, 434, 436.7, and 437.3 nm, respectively. The corresponding dipole strengths are 8, 18, 35, and 35 D^2, giving a total dipole strength of 26 and 70 D^2 for the Soret bands of heme *d* and heme b_{595}, respectively. The interaction energies were calculated using a point dipole approximation. The site inhomogeneity was modeled by uncorrelated shifts of the transition energies. The shifts were randomly taken from a Gaussian distribution with the width (fwhm) of σ = 580 cm^{-1}. The line widths are determined by inhomogeneous broadening due to disorder and homogeneous broadening due to bath-induced dephasing and relaxation of higher exciton levels. The inhomogeneous broadening has been taken into account explicitly by Monte Carlo averaging over realizations of the disorder. The homogeneous broadening has been described by Gaussians with the widths (fwhm) $\Delta\omega_{1-4}$, of 400, 680, 820, and 950 cm^{-1} for the four exciton levels originating in mixing of the two B_{00} transitions of each heme b_{595} and heme *d*. Line width increases for higher exciton levels are a well-known feature of molecular aggregates (*54*, *55*).

Electronic Transitions in the Dithionite-Reduced E445A Mutant. In the dithionite-reduced E445A mutant, heme b_{595} remains oxidized. Absorption characteristics of ferric b_{595} have not been resolved so far, but its Soret absorption band must be strongly blue-shifted relative to the ferrous state. Accordingly, the excitonic mixing between ferrous heme b_{595} and ferrous heme *d* must be broken in the mutant enzyme. The Soret band of the ferric b_{595} has been approximated provisionally by the B_x and B_y transitions centered at 405 and 407 nm, as suggested by the broad trough centered near 406 nm in the difference spectrum in Figure 1B. The dipole strength of the $B_{x,y}$ transitions in oxidized heme b_{595} has been assumed to be 1.25-fold larger than in the reduced form by analogy with myoglobin.

The four electronic transitions, ω_{1-4}, of heme b^{3+}_{595} and heme d^{2+} in the E445A mutant now group in two essentially noninteracting B_x-B_y pairs, where the two higher energy components, $\omega_{3,4}$, originate from the B_x and B_y transitions of ferric heme b_{595}. Because of enhanced spin-orbital interactions in the oxidized form of heme b_{595}, its electronic transitions, $\omega_{3,4}$, should interact much more strongly with the surroundings as compared to the ferrous form of the heme and, hence, will manifest increased broadening, both homogeneous and inhomogeneous. In order to fit the experimental difference spectrum (dithionite-reduced wild type minus dithionite-reduced E445A), the $\Delta\omega_{3,4}$ values of 1800 and 2100 cm^{-1} were chosen for ferric heme b_{595} in the E445A mutant and an inhomogeneous width of σ = 1700 cm^{-1}. The strong inhomogeneity produces a broad absorption band, determined by the B_x and B_y transitions floating within the region between 400 and 410 nm due to the disorder-induced shifts.

Fitting the Experimental Difference Spectrum (wild type minus E445A). Orientations of the electronic transitions in the heme b_{595}/heme *d* pair are given by the angles (φ_d θ_d γ_d) and (φ_b θ_b γ_b) as shown in Figure 3. According to (*56*), the angle between the porphyrin planes of heme *d* and heme b_{595} is about 35° (heme *d* is perpendicular to the membrane plane, whereas heme b_{595} form an angle of 55° with this plane). Supposing that *z*-axis in Figure 3 is normal to the membrane plane, we assume $\theta_d = 0°$ and $\theta_b = -35°$. Other angles were varied.

Many configurations were tested in the calculations and the results compared. Good fits to the experimental data were found for each of the following configurations, i.e., the results were rather insensitive to relative position of the two hemes. For the configuration shown in Figure 3 (i.e., $\{R_x\ R_y\ R_z\}$ = {1 0 0} with the center-to-center line in the membrane plane) a good fit to experimental spectra is obtained for:

(a) tail-to-tail configuration: (φ_d θ_d γ_d) = (0°, 0°, 90°); (φ_b θ_b γ_b) = (0°, −35°, 90°);

(b) plane-to-plane configuration: (φ_d θ_d γ_d) = (120°, 0°, −65°); (φ_b θ_b γ_b) = (60°, −35°, −65°);

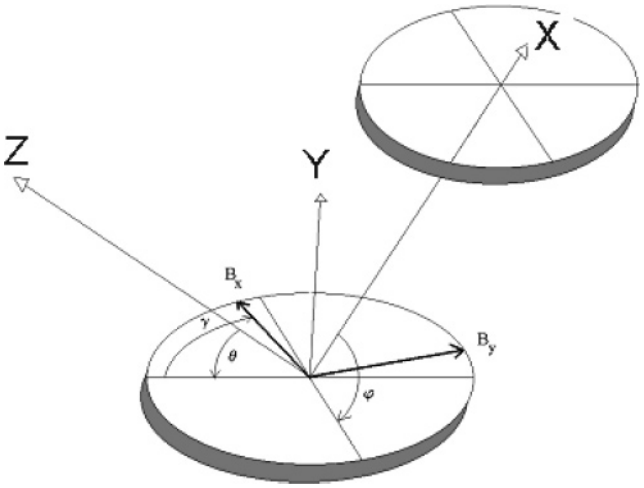

FIGURE 3: Orientations of the heme planes and the B_x and B_y electronic transitions in the heme *d*-heme b_{595} paired hemes.

(c) intermediate configuration: $(\varphi_d\ \theta_d\ \gamma_d) = (0°, 0°, -65°)$; $(\varphi_b\ \theta_b\ \gamma_b) = (-45°, -35°, -65°)$.

For $\{R_x\ R_y\ R_z\} = \{0\ 0\ 1\}$ with the center-to-center line normal to the membrane plane, good fits could also be obtained with the following configurations.

(a) parallel planes configuration: $(\varphi_d\ \theta_d\ \gamma_d) = (0°, 0°, -45°)$; $(\varphi_b\ \theta_b\ \gamma_b) = (0°, -35°, -45°)$;

(b) perpendicular planes configuration: $(\varphi_d\ \theta_d\ \gamma_d) = (45°, 0°, -65°)$; $(\varphi_b\ \theta_b\ \gamma_b) = (-45°, -35°, -65°)$.

Many other intermediate orientations have been checked, and most of them also resulted in good fits to the experimental data. Thus, the Soret band characteristics of the interacting heme b^{2+}_{595}/heme d^{2+} pair are fairly insensitive to relative orientation of the chromophores. This is not surprising, since there are two perpendicular in-plane transitions in each of the two hemes, so that for every orientation, there will be at least one pair of strongly interacting transitions to account for the exciton splitting inherent in the experimental CD and absorption spectra of the wild type enzyme. This circumstance makes it difficult to extract from the fitting the relative orientations of the planes of heme b_{595} and heme *d*, but at the same time it simplifies the determination of the distance between the heme centers.

Fitting not only the absorption line shape but also the absolute values of the CD difference spectrum yields a reliable estimation of the center-to-center distance between heme b_{595} and heme *d*. For any of the configurations, the distance is 9.5 Å to 10.2 Å. Increasing the assumed dipole strength of ferrous heme b_{595} to the highest level of 125 D^2 increases the upper limit to 13−15 Å, and decreasing the assumed dipole strength to the lower limit of 40 D^2 reduces the distance to 7−8 Å.

An example of the fit for the absorption and CD spectra is shown in Figure 4. It can be seen that the modeled curve represents reasonably well the basic features of the Soret absorption band. The main peak of the difference absorption spectrum near 440 nm (panel A) is determined by the overlap of the 436.2 and 441.0 nm components corresponding to the B_x and B_y transitions of heme b^{2+}_{595}. In the unperturbed state, these transitions are located at 436.7 and 437.3 nm, but they are split due to the exciton interaction within the heme b^{2+}_{595}/heme d^{2+} coupled pair and shift further due to energetic disorder. The shoulder on the blue side of the 440 nm peak

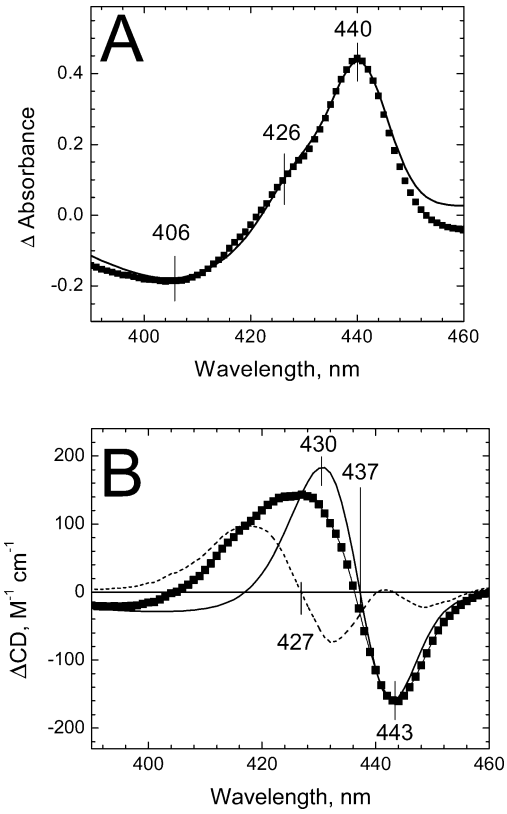

FIGURE 4: Fittings of the absorption difference spectra (Panel A) and CD difference spectra (Panel B) of the dithionite-reduced wild type cytochrome *bd* and E445A mutant. Symbols are experimental data. Solid lines are calculated spectra. The four exciton components in the spectrum of the wild type have maxima at 441.0, 436.2, 431.5, and 426.0 nm. In the mutant, the four transitions center at 434.7, 427.2, 410.6, and 399.2 nm. The dotted line in Figure 4B shows the residual excitonic-type signal, not included in the modeling. The parameters used for the modeling were $\{R_x\ R_y\ R_z\} = \{1\ 0\ 1\}/\sqrt{2}$; center-to-center distance between the two hemes, R = 1.0 nm; orientations $(\varphi_d\ \theta_d\ \gamma_d) = (45°, 0°, -50°)$ and $(\varphi_b\ \theta_b\ \gamma_b) = (100°, -35°, -45°)$.

of ferrous heme b_{595}, first noticed in ref *27*, is assigned as the B_y transition of heme d^{2+}, shifted from 434 to 431.5 nm due to excitonic interactions and disorder. The negative broad band around 406 nm reflects contributions of the B_x and B_y transitions of oxidized heme b_{595} in the mutant.

The calculated difference CD (panel B) reproduces quite accurately the line shape and absolute value of the negative lobe at 443 nm of the measured spectrum. Below the zero crossing point at 437 nm, the experimental curve deviates from the symmetrical positive image of the negative lobe, which must be due to a contribution to the CD spectrum in addition to the modeled heme b^{2+}_{595}/heme d^{2+} excitonic splitting. The difference between the experimental and modeled CD spectra is shown in Figure 4B by a dotted line and gives a derivative-shaped curve with a peak-to-trough amplitude of almost 200 M^{-1} cm^{-1} with a zero-crossing point near 427 nm. This feature may reflect additional excitonic interactions in the wild type cytochrome *bd* involving vibronic components of the Soret bands of the hemes b^{2+}_{595} and d^{2+}; these vibronic components have not been included in our model, as they are not clearly resolved in the absorption spectra, but they may be expected within some 7−10 nm to the blue from the corresponding purely electronic B_{00} transitions, i.e., around 427 nm. It is noted that the additional interactions between the vibronic com-

ponents will not significantly affect our estimation of the heme *d*-to-heme b_{595} distance based on the consideration of the excitonic interaction between the purely electronic B_{00} transitions.

CONCLUSIONS

These data provide direct and reliable evidence for the physical proximity of heme *d* and heme b_{595} in cytochrome *bd* and yield a distance between these redox centers. The spatial proximity provides a simple explanation for the experimentally observed functional interactions between the two hemes such as the negative cooperativity in ligand binding (*31*), redox coupling of the two hemes to the same ionizable groups (*33*), and the migration of CO within the protein from heme *d* to heme b_{595} at cryogenic temperatures (*25*).

However, the center-to-center distance of 10 Å is significantly larger than the 4−5 Å observed for the Fe/Cu_B pair in the heme-copper oxidases. Hence, it is probably not correct to speak about the "binuclear oxygen-reducing site" in cytochrome *bd* and imply that heme b_{595} is a functional counterpart of Cu_B (cf. a similar note in (*1*)). The distance of 10 Å is also probably too large to allow for magnetic coupling between the two hemes, in contrast to the spin-coupled high-spin heme/Cu_B pair in the heme-copper oxidases. A plausible function for heme b_{595}, apart from electron delivery to heme *d* or to heme *d*-bound oxygen intermediates, might consist of providing a binding site for hydroxide formed from heme *d*-bound oxygen upon reductive splitting of the O−O bond.

REFERENCES

1. Junemann, S. (1997) Cytochrome *bd* terminal oxidase, *Biochim. Biophys. Acta 1321*, 107−127.
2. Tsubaki, M., Hori, H., and Mogi, T. (2000) Probing molecular structure of dioxygen reduction site of bacterial quinol oxidases through ligand binding to the redox metal centers, *J. Inorg. Biochem. 82*, 19−25.
3. Poole, R. K., and Cook, G. M. (2000) Redundancy of aerobic respiratory chains in bacteria? Routes, reasons and regulation, *Adv. Microbiol. Physiol. 43*, 165−224.
4. Koland, J. G., Miller, M. J., and Gennis, R. B. (1984) Reconstitution of the Membrane-Bound, Ubiquinone-Dependent Pyruvate Oxidase Respiratory Chain of *Escherichia coli* with the Cytochrome *d* Terminal Oxidase, *Biochemistry 23*, 445−453.
5. Puustinen, A., Finel, M., Haltia, T., Gennis, R. B., and Wikstrom, M. (1991) Properties of the Two Terminal Oxidases of *Escherichia coli*, *Biochemistry 30*, 3936−3942.
6. Bertsova, Y. V., Bogachev, A. V., and Skulachev, V. P. (1997) Generation of protonic potential by the *bd*-type quinol oxidase of *Azotobacter vinelandii*, *FEBS Lett. 414*, 369−372.
7. Kolonay, J. F., Jr, and Maier, R. J. (1997) Formation of pH and potential gradients by the reconstituted *Azotobacter vinelandi* cytochrome *bd* respiratory protection oxidase, *J. Bacteriol. 179*, 3813−3817.
8. Kelly, M. J.S., Poole, R. K., Yates, M. G., and Kennedy, C. (1990) Cloning and Mutagenesis of Genes Encoding the Cytochrome *bd* Terminal Oxidase Complex in *Azotobacter Vinelandii*: Mutants Deficient in the Cytochrome *d* Complex Are Unable to Fix Nitrogen in Air, *J. Bacteriol. 172*, 6010−6019.
9. Hill, S., Viollet, S., Smith, A. T., and Anthony, C. (1990) Roles for Enteric *d*-Type Cytochrome Oxidase in N_2 Fixation and Microaerobiosis, *J. Bacteriol. 172*, 2071−2078.
10. Baughn, A. D., and Malamy, M. H. (2004) The strict anaerobe *Bacteroides fragilis* grows in and benefits from nanomolar concentrations of oxygen, *Nature 427*, 441−444.
11. Smith, A., Hill, S., and Anthony, C. (1990) The Purification, Characterization and Role of the *d*-Type Cytochrome Oxidase of *Klebsiella Pneumoniae* During Nitrogen Fixation, *J. Gen. Microbiol. 136*, 171−180.
12. D'Mello, R., Hill, S., and Poole, R. K. (1994) Determination of the Oxygen Affinities of Terminal Oxidases in *Azotobacter vinelandii* Using the Deoxygenation of Oxyleghaemoglobin and Oxymyoglobin: Cytochrome *bd* is a Low-affinity Oxidase, *Microbiology 140*, 1395−1402.
13. Kaminski, P. A., Kitts, C. L., Zimmerman, Z., and Ludwig, R. A. (1996) *Azorhizobium caulinodans* uses both cytochrome *bd* (quinol) and cytochrome cbb3 (cytochrome c) terminal oxidases for symbiotic N2 fixation, *J. Bacteriol. 178*, 5989−5994.
14. Poole, R. K., and Hill, S. (1997) Respiratory protection of nitrogenase activity in *Azotobacter vinelandii* - roles of the terminal oxidases, *Biosci. Rep. 17*, 307−317.
15. Shi, L., Sohaskey, C. D., Kana, B. D., Dawes, S., North, R. J., Mizrahi, V., and Gennaro, M. L. (2005) Changes in energy metabolism of *Mycobacterium tuberculosis* in mouse lung and under *in vitro* conditions affecting aerobic respiration, *Proc. Natl. Acad. Sci. U.S.A. 102*, 15629−15634.
16. Way, S. S., Sallustio, S., Magliozzo, R. S., and Goldberg, M. B. (1999) Impact of either Elevated or Decreased Levels of Cytochrome *bd* Expression on *Shigella flexneri* Virulence, *J. Bacteriol. 181*, 1229−1237.
17. Endley, S., McMurray, D., and Ficht, T. A. (2001) Interruption of the *cyfB* Locus in *Brucella abortus* Attenuates Intracellular Survival and Virulence in the Mouse Model of Infection, *J. Bacteriol. 183*, 2454−2462.
18. Loisel-Meyer, S., Jimenez, de Bagues, M. P., Kohler, S., Liautard, J. P., and Jubier-Maurin, V. (2005) Differential use of the two high-oxygen-affinity terminal oxidases of Brucella suis for in vitro and intramacrophagic multiplication., *Infect. Immun. 73*, 7768−7771.
19. Yamamoto, Y., Poyart, C., Trieu-Cuot, P., Lamberet, G., Gruss, A., and Gaudu, P. (2005) Respiration metabolism of Group B Streptococcus is activated by environmental haem and quinone and contributes to virulence., *Mol. Microbiol. 56*, 525−534.
20. Zhang-Barber, L., Turner, A. K., Martin, G., Frankel, G., Dougan, G., and Barrow, P. A. (1997) Influence of Genes Encoding Proton-Translocating Enzymes on Suppression of *Salmonella typhimurium* Growth and Colonization, *J. Bacteriol. 179*, 7186- 7190.
21. Zhang, J., Barquera, B., and Gennis, R. B. (2004) Gene fusions with β -lactamase show that subunit I of the cytochrome *bd* quinol oxidase from *E. coli* has nine transmembrane helices with the O_2 reactive site near the periplasmic surface, *FEBS Lett. 561*, 58−62.
22. Poole, R. K., and Williams, H. D. (1987) Proposal that the Function of the Membrane-bound Cytochrome a_1-like Haemoprotein (Cytochrome *b*-595) in *Escherichia coli* is a Direct Electron Donation to Cytochrome *d*, *FEBS Lett. 217*, 49−52.
23. Kobayashi, K., Tagawa, S., and Mogi, T. (1999) Electron Transfer Process in Cytochrome *bd*-type Ubiquinol Oxidase from *Escherichia coli* revealed by Pulse Radiolysis, *Biochemistry 38*, 5913−5917.
24. Rothery, R. A., Houston, A. M., and Ingledew, W. J. (1987) The Respiratory Chain of Anaerobically Grown *Escherichia coli*: Reactions with Nitrite and Oxygen, *J. Gen. Microbiol. 133*, 3247−3255.
25. Hill, J. J., Alben, J. O., and Gennis, R. B. (1993) Spectroscopic Evidence for a Heme-heme Binuclear Center in the Cytochrome *bd* Ubiquinol Oxidase from *Escherichia coli*, *Proc. Natl. Acad. Sci. U.S.A. 90*, 5863−5867.
26. Krasnoselskaya, I., Arutjunjan, A. M., Smirnova, I., Gennis, R., and Konstantinov, A. A. (1993) Cyanide-reactive Sites in Cytochrome *bd* Complex from *E. coli*, *FEBS Lett. 327*, 279−283.
27. Vos, M. H., Borisov, V. B., Martin, J.-L., and Konstantinov, A. A. (2000) Femtosecond resolution of ligand-heme interactions in the high-affinity quinol oxidase *bd*: A di-heme active site?, *Proc. Natl. Acad. Sci. U.S.A. 97*, 1554−1559.
28. Borisov, V. B., Liebl, U., Rappaport, F., Martin, J.-L., Zhang, J., Gennis, R., Konstantinov, A., and Vos, M. H. (2002) Interactions between Heme *d* and Heme b_{595} in Quinol Oxidase *bd* from *Escherichia coli*: A Photoselection Study Using Femtosecond Spectroscopy, *Biochemistry 41*, 1654−1662.
29. Hori, H., Tsubaki, M., Mogi, T., and Anraku, Y. (1996) EPR Study of NO Complex of *bd*-type Ubiquinol Oxidase from *Escherichia coli*, *J. Biol. Chem. 271*, 9254−9258.
30. Borisov, V. B., Sellednikova, S. E., Poole, R. E., and Konstantinov, A. A. (2001) Interaction of cytochrome *bd* with carbon monoxide at low and room temperatures, *J. Biol. Chem. 276*, 22095−22099.

31. Borisov, V., Arutyunyan, A. M., Osborne, J. P., Gennis, R., and Konstantinov, A. A. (1999) Magnetic Circular Dichroism Used to Examine the Interaction of *Escherichia coli* cytochrome *bd* with ligands, *Biochemistry 38*, 740−750.
32. Borisov, V. B., Gennis, R. B., and Konstantinov, A. A. (1995) Interaction of cytochrome *bd* from *Escherichia coli* with hydrogen peroxide, *Biochemistry (Moscow*) *60*, 231−239 231−239 (Translated from Biokhimiya (in Russian) (1995) *60*, 315−327).
33. Belevich, I., Borisov, V. B., Zhang, J., Yang, K., Konstantinov, A. A., Gennis, R. B., and Verkhovsky, M. I. (2005) Time-resolved electrometric and optical studies on cytochrome *bd* suggest a mechanism of electron-proton coupling in the di-heme active site, *Proc. Natl. Acad. Sci. U.S.A. 102*, 3657−3662.
34. Zhang, J., Hellwig, P., Osborne, J. P., Huang, H.-w., Moenne-Loccoz, P., Konstantinov, A. A., and Gennis, R. B. (2001) Site-directed mutation of the highly conserved region near the Q-loop of cytochrome *bd* quinol oxidase from *Escherichia coli* specifically perturbs heme b_{595}, *Biochemistry 40*, 8548−8556.
35. Kaysser, T. M., Ghaim, J. B., Georgiou, C., and Gennis, R. B. (1995) Methionine-393 Is an Axial Ligand of the Heme b_{558} Component of the Cytochrome *bd* Ubiquinol Oxidase from *Escherichia coli*, *Biochemistry 34*, 13491−13501.
36. Miller, M. J., and Gennis, R. B. (1986) Purification and reconstitution of the cytochrome *d* terminal oxidase complex from *Escherichia coli*, *Methods Enzymol. 126*, 87−94.
37. Koland, J. G., Miller, M. J., and Gennis, R. B. (1984) Reconstitution of the membrane-bound, ubiquinol-dependent pyruvate oxidase respiratory chaine of *Escherichia coli* with the cytochrome *d* terminal oxidase, *Biochemistry 23*, 7933−7935.
38. Lorence, R. M., Koland, J. G., and Gennis, R. B. (1986) Coulometric and Spectroscopic Analysis of the Purified Cytochrome *d* Complex of *Escherichia coli*: Evidence for the Identification of "Cytochrome a_1" as Cytochrome b_{595}, *Biochemistry 25*, 2314−2321.
39. Myer, Y. P. (1985) *Circular Dichroism Studies of Electron Transfer Components*, Vol. 14, pp 149−188, Academic Press, New York.
40. Palmer, G., and Esposti, M. D. (1994) Application of Exciton Coupling Theory to the Structure of Mitochondrial Cytochrome *b*, *Biochemistry 33*, 176−185.
41. Sono, M., Bracete, A. M., Huff, A. M., Ikeda-Saito, M., and Dawson, J. H. (1991) Evidence That a Formyl-substituted Iron Porphyrin is the Prosthetic Group of Myeloperoxidase: Magnetic Circular Dichroism Similarity of the Peroxidase to *Spirographis* Heme-reconstituted Myoglobin, *Proc. Natl. Acad. Sci. U.S.A. 88*, 11148−11152.
42. Bracete, A. M., Kadkhodayan, S., Sono, M., Huff, A. M., Zhuang, C., Cooper, D. K., Smith, K. S., Chang, C. K., and Dawson, J. H. (1994) Iron Chlorin-reconstituted Histidine-Ligated Heme Proteins as Models for Naturally Occuring Iron Chlorin Proteins: Magnetic Circular Dichroism Spectroscopy as a Probe of Iron Chlorin Coordination Structure, *Inorg. Chem. 33*, 5042−5049.
43. Hsu, M.-C., and Woody, R. W. (1971) The origin of the heme Cotton effects in myoglobin and hemoglobin, *J. Am. Chem. Soc. 93*, 3515−3525.
44. Arutyunyan, A. M., and Denisenko, A. N. (1986) Manifestation of heme-heme interaction in circular dichroism spectra, *Mol. Biol. (Moscow) (Engl. Transl.) 20*, 514−518.
45. Blauer, G., Sreerama, N., and Woody, R. W. (1993) Optical activity of hemoproteins in the Soret region. Circular dichroism of the heme undecapeptide of cytochrome *c* in aqueous solution, *Biochemistry 32*, 6674−6679.
46. Goldbeck, R. A., Sagle, L., Kim-Shapiro, D. B., Flores, V., and Kliger, D. S. (1997) Evidence for heme-heme excitonic coupling in the Soret Circular Dichroism of Hemoglobin, *Biochem. Biophys. Res. Commun. 235*, 610−614.
47. Nicola, N. A., Minasian, E., Appleby, C. A., and Leach, S. J. (1975) Circular dichroism studies of myoglobin and leghemoglobin, *Biochemistry 14*, 5141−5149.
48. Degli Esposti, M., Kamensky, Y. A., Arutjunjan, A. M., and Konstantinov, A. A. (1989) A Model for Molecular Organization of Cytochrome *b*-561 in Chromaffin Granule Membranes, *FEBS Lett. 254*, 74−78.
49. Esposti, M. D., Crimi, M., Kortner, C., Kroger, A., and Link, T. (1991) The Structure of the Dihaem Cytochrome *b* of Fumarate Reductase in *Wolinella Succinogenes*: Circular Dichroism and Sequence Analysis Studies, *Biochim. Biophys. Acta 1056*, 243−249.
50. Degli Esposti, M., Palmer, G., and Lenaz, G. (1989) Circular Dichroic Spectroscopy of Membrane Haemoproteins. The Molecular Determinants of the Dichroic Properties of the *b* cytochromes in Various Ubiquinol:Cytochrome *c* reductases, *Eur. J. Biochem. 182*, 27−36.
51. Schoepp, B., Chabaud, E., Breyton, C., Vermeglio, A., and Popot, J.-L. (2000) On the Spatial Organization of Hemes and Chlorophyll in Cytochrome b_6f. A linear and Circular Dichroism Study, *J. Biol. Chem. 275*, 5275−5283.
52. Sherz, A., and Parson, W. W. (1984) Exciton interaction sin dimers of bacteriochlorophyl and related molecules., *Biochim. Biophys. Acta 766*, 666−678.
53. Coulter, E. D., Cheek, J., Ledbetter, A. P., Chang, C. K., and Dawson, J. H. (2000) Preparation and initial characterization of the compound I, II, and III states of iron methylchlorin-reconstituted horseradish peroxidase and myoglobin: models for key intermediates in iron chlorin enzymes, *Biochem. Biophys. Res. Commun. 279*, 1011−1015.
54. Kuhn, O., and Sundstrom, V. (1997) Pump-probe spectroscopy of dissipative energy transfer dynamics in photosynthetic antenna complexes: A density matrix approach, *J. Chem. Phys. 107*, 4154−4164.
55. Novoderezhkin, V., and van Grondelle, R. (2002) Exciton-vibrational relaxation and transient absorption dynamics in LH1 of *Rhodopseudomonas viridis*: a Redfield theory approach., *J. Phys. Chem. Biol. 106*, 6025−6037.
56. Ingledew, W. J., Rothery, R. A., Gennis, R. B., and Salerno, J. C. (1991) The Orientation of the Three Haems of the *in situ* Ubiquinol Oxidase, Cytochrome *bd* of *Escherichia coli*, *Biochem. J. 282*, 255−259.

BI701884G